Environmental Science & Technology

Article

pubs.acs.org/est

A Flux-Gradient System for Simultaneous Measurement of the CH_4, CO_2, and H_2O Fluxes at a Lake–Air Interface

Wei Xiao,[†,‡] Shoudong Liu,[†,‡] Hanchao Li,[†] Qitao Xiao,[§] Wei Wang,[†] Zhenghua Hu,[†] Cheng Hu,[†] Yunqiu Gao,[†] Jing Shen,[†] Xiaoyan Zhao,[§] Mi Zhang,[†] and Xuhui Lee*[,†,⊥]

[†]Yale-NUIST Center on Atmospheric Environment, [‡]Collaborative Innovation Center on Forecast and Evaluation of Meteorological Disasters, and [§]Jiangsu Key Laboratory of Agricultural Meteorology, Nanjing University of Information Science & Technology, Nanjing, Jiangsu 210044, China

[⊥]School of Forestry and Environmental Studies, Yale University, New Haven, Connecticut 06511, United States

Supporting Information

ABSTRACT: Inland lakes play important roles in water and greenhouse gas cycling in the environment. This study aims to test the performance of a flux-gradient system for simultaneous measurement of the fluxes of water vapor, CO_2, and CH_4 at a lake–air interface. The concentration gradients over the water surface were measured with an analyzer based on the wavelength-scanned cavity ring-down spectroscopy technology, and the eddy diffusivity was measured with a sonic anemometer. Results of a zero-gradient test indicate a flux measurement precision of 4.8 W m^{-2} for water vapor, 0.010 mg m^{-2} s^{-1} for CO_2, and 0.029 μg m^{-2} s^{-1} for CH_4. During the 620 day measurement period, 97%, 69%, and 67% of H_2O, CO_2, and CH_4 hourly fluxes were higher in magnitude than the measurement precision, which confirms that the flux-gradient system had adequate precision for the measurement of the lake–air exchanges. This study illustrates four strengths of the flux-gradient method: (1) the ability to simultaneously measure the flux of H_2O, CO_2, and CH_4; (2) negligibly small density corrections; (3) the ability to resolve small CH_4 gradient and flux; and (4) continuous and noninvasive operation. The annual mean CH_4 flux (1.8 g CH_4 m^{-2} $year^{-1}$) at this hypereutrophic lake was close to the median value for inland lakes in the world (1.6 g CH_4 m^{-2} $year^{-1}$). The system has adequate precision for CH_4 flux for broad applications but requires further improvement to resolve small CO_2 flux in many lakes.

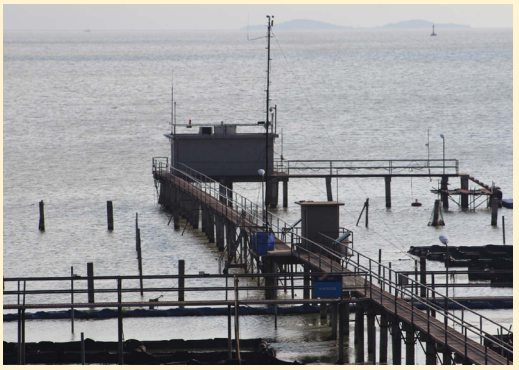

1. INTRODUCTION

Inland waters such as lakes and reservoirs are important components of the global greenhouse gas cycles.[1−5] The fluxes of these gases when expressed on the unit surface area basis are however very small. Measuring these fluxes is challenging because of small signal-to-noise ratios. Several measurement techniques are available, and each has its advantages and disadvantages.[6−8] The most common methods are floating chamber and water equilibrium methods. Floating chambers are relatively simple to operate, and the measurement uncertainties are not noticeable if designed properly.[9−11] However, it can only represent small areas since the footprint is small.[11] Additionally, they are difficult to deploy in high wind conditions, and high frequency measurements are labor-intensive.[7] The water equilibrium method determines the flux by measuring the concentration difference between the surface water and the air layer above.[12−14] It can be used in remote locations and at multiple sites. A major limitation is the uncertainty introduced by the diffusivity coefficient, especially in low wind (<5 m s^{-1}) and high wind (>10 m s^{-1}) conditions.[15] Furthermore, the water equilibrium method cannot capture CH_4 ebullition, which can be a large component of the CH_4 flux in lakes.[5,16]

Micrometeorological methods measure the water–air flux continuously and noninvasively using instruments placed in the atmospheric surface layer over the water surface. Eddy covariance (EC) has been increasingly used to measure the CO_2 flux at lake–air interfaces.[7,17−19] Several researchers have also deployed the EC method to measure the CH_4 flux.[8,20,21] However, if not treated carefully, measurement artifacts, such as error propagation through the density corrections,[7,22,23] motion of the measuring platform,[7,24−26] and artificial density fluctuations from sensor self-heating of open-path sensors,[27] can overwhelm the small flux signal.

The flux-gradient (FG) technique, another micrometeorological method, determines the flux as the vertical concentration gradient multiplied by an eddy diffusivity.[28] The FG method is also noninvasive and can be used continuously. For example, it was used to measure the CO_2 and H_2O fluxes at Lake Gårdsjön, Sweden more or less continuously for 14 days[29] and CO_2 and CH_4 fluxes between a boreal beaver pond and the atmosphere

Received: August 29, 2013
Revised: October 23, 2014
Accepted: November 7, 2014
Published: November 7, 2014

dx.doi.org/10.1021/es5033713 | Environ. Sci. Technol. 2014, 48, 14490−14498

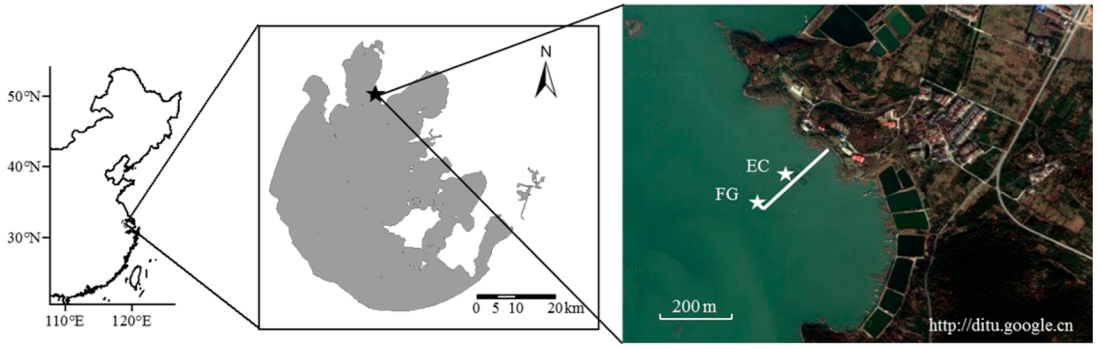

Figure 1. Map showing the experimental site at Lake Taihu. Locations of the FG and EC instruments are indicated by the star symbols. The white lines mark a boardwalk (width 1 m) at 2 m above the water surface.

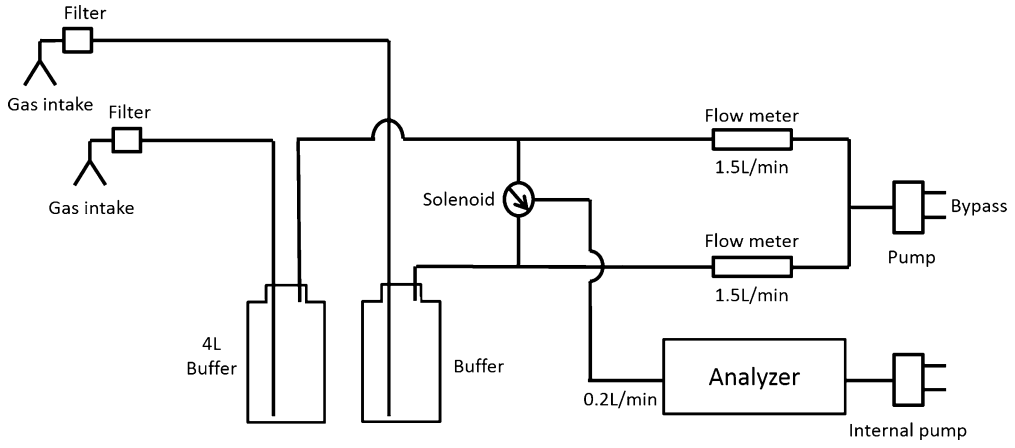

Figure 2. Schematic design diagram of the gradient measurement system.

continuously for 4 months.[30] An advantage of the FG method (and also the EC method) with a closed-path analyzer over open-path EC is that its density corrections are much smaller. However, gaseous concentration gradients are very small in the atmospheric surface layer over lakes, and the difficulty for conventional instruments to resolve the gradient signals has limited the deployment of the FG method to short field campaigns. For example, the vertical variations in the CO_2 concentration over a lake are on the order of 1 ppm or less, which is near the measurement precision of some broadband infrared analyzers. To obtain defensible gradient data, Zappa et al.[31] compensated the short-term signal drifts of their broadband infrared analyzer by drawing air into one analyzer from multiple heights using a moving inlet and by having a second analyzer measuring the background concentration at a fixed height.

The FG method involves parametrization of the eddy diffusivity K in the atmospheric surface layer. The K parametrization[32] has been successfully deployed for flux observations in terrestrial ecosystems,[33] but to the best of the authors' knowledge, extensive testing of this method for lake systems has not yet been reported in the published literature. In the terrestrial environment, K is well-behaved in unstable conditions,[32,34] usually in the daytime, with fully developed turbulence, but at these times, the vertical concentration gradient is small and difficult to measure. At night, the gradient may be larger, but K may be uncertain especially if the atmosphere becomes very stable. The situation can be different over a lake where unstable air can actually occur at night if water is warmer than the overlaying air.

In this study, a wavelength-scanned cavity ring-down spectroscopy (WS-CRDS) trace gas analyzer was deployed in the FG mode to measure the H_2O, CO_2, and CH_4 fluxes at a lake−atmosphere interface. In recent years, WS-CRDS analyzers have been used increasingly in measurements of atmospheric CO_2 and CH_4 concentrations.[35−38] However, these analyzers have not yet been used in the gradient mode for surface flux measurements. WS-CRDS analyzers can measure the gaseous concentration without the need to dry the air.[36,39,40] They have ability to measure the water vapor mixing ratio (and its flux) simultaneously with the trace gases, which is a feature useful for checking the eddy diffusivity calculations with the modified Bowen-ratio (MBR) approach[29,31,41] and for surface evaporation and energy balance studies. During the experimental period in this study, the analyzer was stable and could resolve the small vertical concentration differences over a water surface. The present study appears to be the first attempt at measuring the H_2O, CO_2, and CH_4 fluxes simultaneously using one instrument and in a long-term operation. The measurement took place at Lake Taihu, China from May 11, 2012 to January 18, 2014. The goal of this paper is to present a performance evaluation of this measurement system.

In addition, the data are used to examine the hypothesis that the measurement site, a shallow and hypereutrophic lake, is a strong source of CH_4 in comparison to other lake systems. A survey of the literature reveals large variations in the measured CH_4 flux in eutrophic lakes (Table S2, Supporting Information). Some of the variations may have been caused by methodological artifacts. The nonintrusive measurement reported here can help narrow the uncertainties.

dx.doi.org/10.1021/es5033713 | Environ. Sci. Technol. 2014, 48, 14490−14498

2. MATERIALS AND METHODS

2.1. Study Site. The experimental site (31°24′ N, 120°13′ E) was located in the northern part of Lake Taihu (area, 2400 km^2; mean depth, 1.9 m; Figure 1) as part of the Taihu Eddy Flux Network.[42] The annual air temperature is 16.2 °C, and annual precipitation is 1122 mm under humid-subtropical climate according to the Köppen climate classification.[42] The most ideal fetch conditions occurred when wind direction fell in the range of 180−270°. In this wind direction range, the measurement was not interfered by land and by the measurement platforms. Lake water at this site was super-eutrophic with abundant phytoplankton growth.[43]

2.2. Flux-Gradient Method. A WS-CRDS analyzer (Model G1301, Picarro Inc., CA, USA) was employed to measure the mixing ratio of CO_2, CH_4, and H_2O at 0.5 Hz. The 5 min precision supplied by the manufacturer for the analyzer is 50 ppb for CO_2, 0.7 ppb for CH_4, and 50 ppm for H_2O. Air was drawn from two air intakes at the heights of 1.1 and 3.5 m above the water surface through unheated Teflon tubings (length, 22 m; tube inner diameter, 0.32 cm) into the analyzer (Figure 2). The intakes were protected by inline air filters (model SS-4FW-7, Swagelok Company, Solon, OH, USA). To improve the gradient measurement, we reduced turbulent fluctuations with buffer volumes (4 L) and minimized the transient time between valve switching using short tubes (length of 0.5 m between the analyzer and the three-way valve). The bypass flow rate of the sampling system was 1.5 L min^{-1}, and a small portion (0.2 L min^{-1}) was subsampled by the analyzer. A pump (D888−12, Parker Hannifin Corporation, NC, USA) was used for bypass. A three-way solenoid valve (model T3NCSS-078, IQ Valves Co., FL, USA) switched between the two intakes every 60 s, and the measurements approached steady state in less than 10 s after each switching. Figure 3 shows the step changes in the CO_2, CH_4, and H_2O mixing ratios in response to valve switching for a 10 min measurement period. During this period, the absolute difference between the two heights was ∼5 ppb for CH_4, ∼1 ppm for CO_2, and ∼0.2 %v for H_2O. These concentration differences were captured by the measurement system. The data were block-averaged to half-hourly means for the flux calculation.

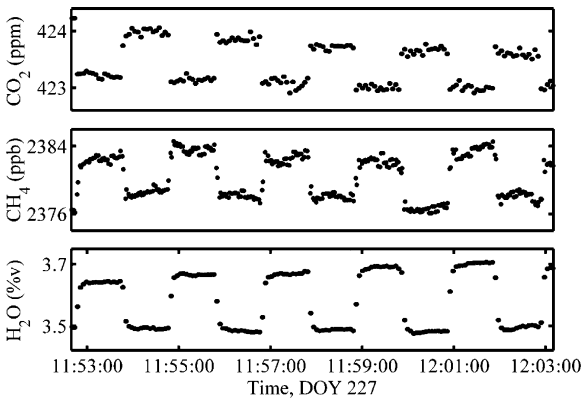

Figure 3. Step changes in the CO_2, CH_4, and H_2O mixing ratios in response to valve switching from around 11:53:00 to 12:03:00 on DOY 227, 2012.

The analyzer was housed in a small building elevated over the water surface, at a linear distance of 250 m away from the shore (Figure 1). Details on the instrument calibration are given in the Supporting Information. The gas intakes were secured, at a distance of 20 m from the instrument building, on a vertical metal pole, which was fastened onto a narrow boardwalk. The peak contribution to the flux footprint[44] in neutral stability was at 102, 22, and 47 m away for the upper intake, lower intake, and the geometric mean of the two intake heights, respectively. To avoid the problem of footprint mismatch, we only analyzed the data collected during times when the wind came from the open water (wind direction 180−270°).

The experiment started in May, 2012. In this study, we analyzed the data collected before January 18, 2014. The fluxes were calculated according to the flux-gradient theory as

$$F = -c\rho_a K \frac{r_2 - r_1}{z_2 - z_1} \quad (1)$$

where F is the flux of CO_2 (mg m^{-2} s^{-1}), CH_4 (μg m^{-2} s^{-1}), or H_2O (g m^{-2} s^{-1}); r_1 and r_2 are the corresponding half-hourly mean dry air mixing ratios (ppm for CO_2, ppb for CH_4, and %v for H_2O) at heights z_1 and z_2 (m); ρ_a is air density (kg m^{-3}); c is a unit conversion constant (44/29 for CO_2, 16/29 for CH_4, and 18/29 for H_2O); and K is eddy diffusivity (m^2 s^{-1}). The eddy diffusivity was calculated with the aerodynamic method:

$$K = ku_* \times z_g/\varphi_h \quad (2)$$

where k is the von Kármán constant; u_* is friction velocity (m s^{-1}); z_g is the geometric mean of the two measurement heights (m), that is, $z_g = (z_1 z_2)^{1/2}$; and φ_h is the Obukhov stability function:[32]

$$\varphi_h = 1 + 5\zeta \quad \text{for } \zeta > 0 \text{ (stable conditions)}$$
$$\varphi_h = (1 - 16\zeta)^{-1/2} \quad \text{for } \zeta \le 0 \text{ (neutral and unstable conditions)} \quad (3)$$

where $\zeta = z_g/L$, and L is the Obukhov length (m). Here, L is given by $L = -u_*^3/[k(g/\theta_v)\overline{w'\theta'}]$, where g is gravity acceleration (9.8 m s^{-2}); θ_v is virtual potential temperature (K); and $\overline{w'\theta'}$ is kinematic sensible heat flux (m K s^{-1}), with u_* and $\overline{w'\theta'}$ determined with an EC system described below.

As pointed out in the Introduction, the simultaneous and accurate measurement of the H_2O mixing ratio allowed us to check the eddy diffusivity calculations by comparing the above aerodynamic method with the MBR approach, both of which assume that the eddy diffusivities for all scalars are the same. In this method, the water vapor was treated as the tracer, and K was calculated using eq 1 from the measured water vapor flux and its concentration difference. The CO_2 and CH_4 fluxes were then determined using eq 1.

2.3. Eddy-Covariance Method. An EC system was secured onto a small concrete pillar at a height of 3.5 m above the water and a distance of 100 m from the FG intakes (Figure 1). Three dimensional wind speeds and air temperature fluctuations were measured with a three-dimensional sonic anemometer/thermometer (model CSAT3, Campbell Scientific Inc., Logan, UT, USA), and atmospheric H_2O and CO_2 concentrations were measured with an open-path infrared gas analyzer (IRGA, model LI7500, Li-Cor Inc., Lincoln, NE, USA). The measurement frequency was 10 Hz. The fluxes of H_2O, CO_2, sensible heat, and momentum were computed at 30 min intervals from the 10 Hz measurement.[45] The fluxes of sensible heat and momentum were used to calculate the eddy diffusivity (eq 2), and the fluxes of H_2O and CO_2 were used to evaluate the performance of the FG system.

Table 1. Mean Value and Standard Deviation of Half-Hourly CO_2, CH_4, and H_2O Mixing Ratio Differences (Lower Intake Minus Upper Intake) and Fluxes, and Eddy Diffusivity during the Zero-Gradient Test

	mixing ratio difference			flux			
	H_2O (%v)	CO_2 (ppm)	CH_4 (ppb)	LE (W m^{-2})	F_c (mg m^{-2} s^{-1})	F_m (μg m^{-2} s^{-1})	K (m^2 s^{-1})
mean value	-7.4×10^{-5}	−0.033	0.20	−0.05	−0.008	0.016	0.31
standard deviation	0.0020	0.041	0.36	4.8	0.010	0.029	0.04

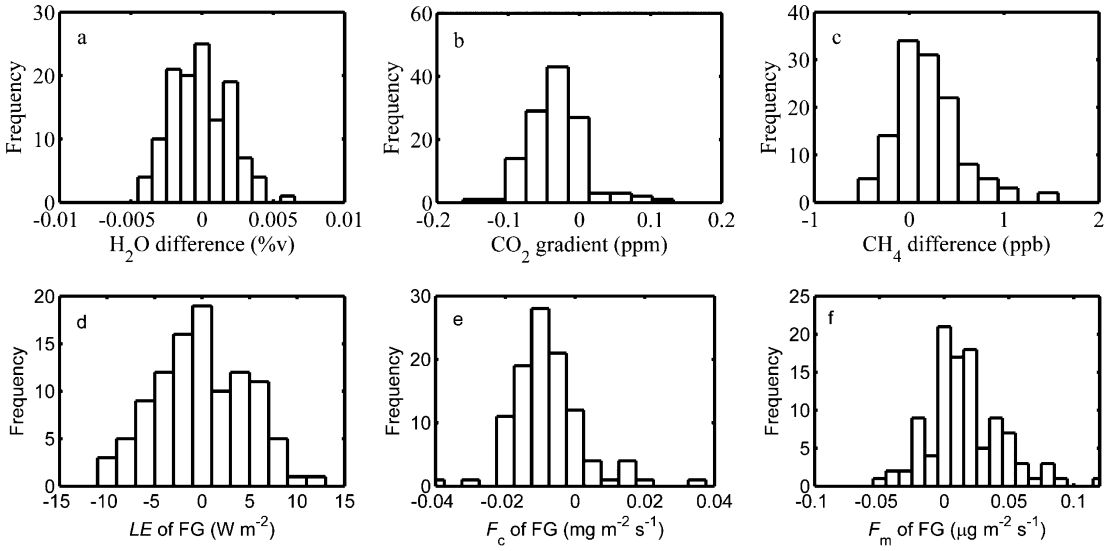

Figure 4. Frequency distribution of the H_2O, CO_2, and CH_4 mixing ratio differences and fluxes obtained from the zero-gradient test.

The eddy fluxes were computed using 30 min block averaging. The flux of CO_2 was determined from $F_c = \overline{w'c'}$, where w' and c' are fluctuations in the vertical velocity and in the CO_2 density, respectively, and the overbar denotes block averaging. Rotation into the natural wind coordinate was performed.[46] The heat and water vapor diffusion in air cause additional density fluctuations of H_2O, CO_2, and CH_4. The effect of fluctuations of heat and water vapor on the flux measurements were corrected using the classic density correction theory of Webb, Pearman, and Leuning (WPL).[47] The density correction to the EC CO_2 flux can be in error because open-path analyzers do not provide precise enough measurement of the mean CO_2 concentration.[48] In the present study, the WPL-corrected infrared gas analyzer (IRGA) CO_2 concentration was on average 6.6% lower compared to the WS-CRDS measurement. This IRGA CO_2 concentration was calibrated against the WS-CRDS CO_2 concentration before the WPL correction.

2.4. Ancillary Measurements. During the early part of the experiment, we conducted a parallel field campaign measuring the isotopic composition of the lake evaporation.[49] A water vapor analyzer (model 911−0004, Los Gatos Research, Mountain View, CA, USA) based on the off-axis integrated cavity output spectroscopy was used to measure the water vapor mixing ratio also at the 1.1 and 3.5 m heights above water surface. The analyzer was calibrated every 3 h against a vapor standard at five concentrations that bracketed the ambient humidity. The water vapor concentration (the sum of $H_2{}^{16}O$, HDO, and $H_2{}^{18}O$) measured with this analyzer was used as an independent check on the quality of the FG measurement.

Other micrometeorological measurements included temperature and relative humidity (model HMP45C, Vaisala Inc., Helsinki, Finland), wind speed and direction (model 03002, R M Young Company, Traverse City, MI, USA), water temperature (model 109-L, Campbell Scientific Inc., Logan, UT, USA), and the four components of the surface radiation balance (model CNR4, Kipp & Zonen B. V., Delft, The Netherlands).

3. RESULTS AND DISCUSSION

3.1. Instrument Performance. *Zero-Gradient Test.* A zero-gradient test was performed to quantify bias errors and measurement precision of the FG system. During the test, the two intakes were positioned next to each other. The test was conducted for 62 h, from 1730 LST, July 22 (DOY 204) to 0700 LST, July 25 (DOY 207), 2012. Results indicate very small bias errors (Table 1, Figure 4). The difference was calculated as the mixing ratio at the intake designated for the lower measurement height minus that for the upper measurement height. For H_2O, the standard deviation of the 30 min concentration difference was 0.0020 %v (20 ppm) (Table 1), which was four orders of magnitude smaller than the mean mixing ratio. Similarly, the standard deviation of the CO_2 and CH_4 concentration differences was four orders of magnitude smaller than their mean mixing ratios. Frequency distributions (Figure 4) indicate that 90% of the zero-gradient observations fell in the range of −0.0033−0.0033 %v for H_2O, −0.09−0.05 ppm for CO_2, and −0.5−0.7 ppb for CH_4.

Latent heat flux (LE), CO_2 flux (F_c), and CH_4 flux (F_m), calculated using data from the zero-gradient test, were very small in magnitude. The mean values (±1 standard deviation) of LE, F_c, and F_m were −0.05 (±4. 8) W m^{-2}, −0.008 (±0.010) mg m^{-2} s^{-1}, and 0.016 (±0.029) μg m^{-2} s^{-1}, respectively. Frequency distributions (Figure 4) indicate that 90% of the zero-gradient flux observations fell in the range of −7.5−7.5 W m^{-2} for LE, −0.021−0.010 mg m^{-2} s^{-1} for F_c, and −0.030−

dx.doi.org/10.1021/es5033713 | Environ. Sci. Technol. 2014, 48, 14490−14498

0.060 μg m^{-2} s^{-1} for F_m. During the zero-gradient test, the mean value and standard deviation of K were 0.31 m^2 s^{-1} and 0.04 m^2 s^{-1}, respectively, with a range of 0.22−0.46 m^2 s^{-1}.

The standard deviations of the concentration difference and flux of the zero-gradient test are a measure of the precision of the sampling system and the analyzer. The precisions of this study compare favorably with other published results. A detection limit of 0.026 μg CH_4 m^{-2} s^{-1} has been reported for a closed-chamber method (0.15 m diameter, 0.30 m head space length, 30 min sampling time interval, 120 min for one chamber-covering period) and 0.60−7.08 μg CH_4 m^{-2} s^{-1} for a Bowen-ratio/energy balance method.[50] The detection limit of concentration differences of the tunable diode laser used by Simpson et al. was 0.2 ppb.[34] In the Meyers et al. study,[29] the CO_2 and H_2O fluxes at lake−air interface were measured with a FG method, and the mean bias and standard deviation of CO_2 and H_2O differences were -0.033 ± 0.026 ppm and $-1.1 \times 10^{-4} \pm 3.2 \times 10^{-4}$ %v, respectively, in their zero-gradient test. The precision of the CH_4 gradient measurement with on-line gas chromatography[30] is 4 ppb. In a study of the CH_4 flux using an EC system,[51] the measurement uncertainty was 0.67 μg CH_4 m^{-2} s^{-1}. The automatic CH_4 chamber described by Duc et al.[52] had a detection limit of 0.053 μg CH_4 m^{-2} s^{-1}. The ability to resolve very small CH_4 flux is a major advantage of the FG system for application over water surfaces.

Comparison of Water Vapor Vertical Gradient. The water vapor difference (lower height minus upper height) measurement of the WS-CRDS analyzer agreed well with that of the vapor isotope analyzer, with a geometric mean regression slope of 0.983 (r = 0.95, p < 0.001; Supporting Information). The bias (WS-CRDS minus isotope analyzer) ranged from −0.054−0.056 %v, with a mean bias value of 0.0002 %v and a standard deviation of 0.012 %v. These bias values are slightly bigger than those of the zero-gradient test.

All the sampling components upstream of the isotope vapor analyzer, including its inlets, inlet filters, sampling tubes, buffer volumes, and manifold, were heated to a temperature 5−10 °C above the ambient to avoid condensation and tube wall effects. The sampling lines of the WS-CRDS analyzer on the other hand were not heated. The comparison of the two water vapor analyzers (Supporting Information) shows that lack of heating did not degrade the water vapor gradient measurement for flux determination. They also confirm that the WS-CRDS analyzer's calibration was quite stable.

Comparison of the Aerodynamic and MBR Methods. One source of uncertainty of the FG method is related to the K parametrization. The stability function (eq 3) is not well behaved if air is either very stable ($\zeta > 0.5$) or very unstable ($\zeta < -1$).[34,53] Additionally, this stability function was measured at a distance of 100 m away from the gradient measurement location (Figure 1). To evaluate the FG performance, we compared the CO_2 and CH_4 fluxes using the aerodynamic formulation and those derived from the MBR method[29,31,41] and found very good agreement (Supporting Information). The index of agreement[54] and coefficient of determination (R^2) were 0.81 and 0.49 for CO_2 and 0.85 and 0.55 for CH_4, respectively. The mean difference was −0.006 mg m^{-2} s^{-1} and 0.005 μg m^{-2} s^{-1}, and the root mean squares error (RMSE) was 0.05 mg m^{-2} s^{-1} and 0.11 μg m^{-2} s^{-1} for CO_2 and CH_4, respectively. The few outliers that deviate from the 1:1 line occurred when the water vapor flux was nearly zero. The results indicate that the 100-m horizontal separation between the EC and FG systems had a minor impact on the FG measurement accuracy. During our experiment, ζ rarely fell outside the range of −0.2−0.2, and the good agreement supports the application of the K parametrization (eq 3), which has been established from experimental studies in the terrestrial environment,[32] in lake−air exchange studies.

Sensitivity of the Eddy Covariance Analyzer. To ensure that the EC−FG comparison was not biased by the EC analyzer's calibration errors, we used a postfield method to correct the LI-7500 analyzer sensitivity or the instrument gain factor against the WS-CRDS measurement. The 30 min mean water vapor and CO_2 mixing ratios measured by the IRGA were compared with the WS-CRDS measurements in a geometric mean regression. The regression yielded a slope (IRGA versus WS-CRDS) of 1.043 and 0.910 for water vapor and CO_2 mixing ratios, respectively, which indicates that the IRGA sensitivity had a high bias for water vapor and a low bias for CO_2. In the following, the fluxes represent the online EC fluxes multiplied by these correction factors.

3.2. Water Vapor Exchange. The FG and EC *LE* measurements were in good agreement (Figure 5a). The

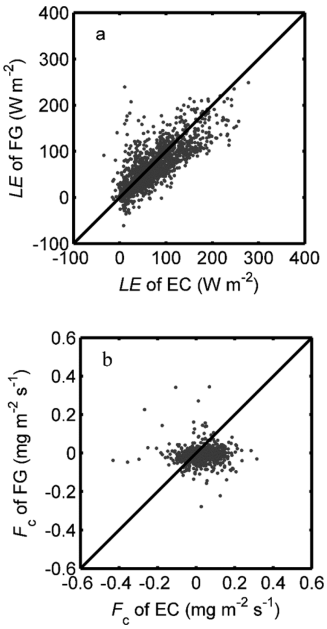

Figure 5. Comparison of latent heat flux (*LE*, a) and CO_2 flux (F_c, b) observed with the EC and the FG methods.

geometric linear regression result is $y = 0.94(\pm 0.03)x - 2.33(\pm 2.13)$ (R^2 = 0.56, n = 1598), where y is the FG flux; x is the EC flux; and the uncertainty ranges on the regression coefficients indicate the 95% confidence bound. The mean difference (ME, FG minus EC) was −6.5 W m^{-2}, with a RMSE value of 36.3 W m^{-2}. The relative bias error (ME divided by the mean flux) was −9%. The index of agreement was 0.86. The frequency distribution (Figure 6a) indicates that 97% of *LE* measured by the FG method was higher than the detection limit obtained from the zero-gradient test (4.8 W m^{-2}). These results show that the FG system was precise enough for the water vapor exchange measurement.

3.3. CO_2 Flux. The EC measurement varied over a broader range than did the FG measurement, with more positive data points (Figure 6b). The mean difference (FG flux minus EC flux) is −0.030 mg m^{-2} s^{-1}, and the RMSE value is 0.087 mg m^{-2} s^{-1}. According to the flux frequency distribution (Figure

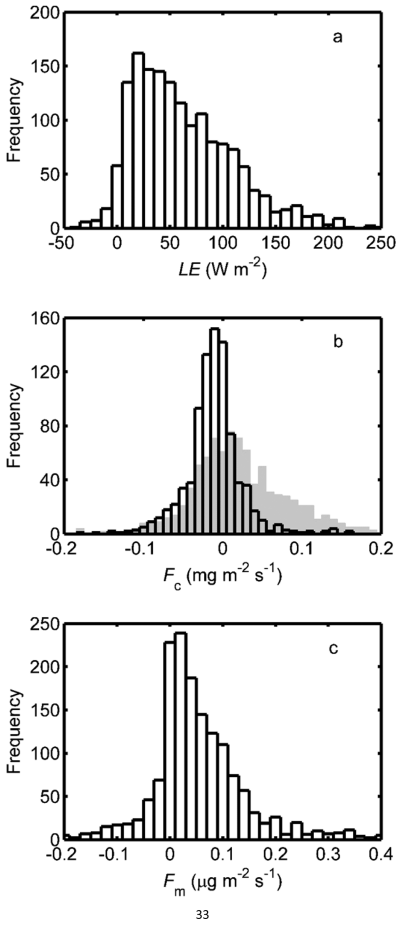

Figure 6. Frequency distribution of the latent heat flux (LE), CO_2 flux (F_c), and CH_4 flux (F_m) measured with the FG method (white columns), and F_c measured with the EC system (gray column).

6b), 69% of the FG observations had F_c magnitude higher than one standard deviation of the F_c measurement during the zero-gradient test (0.010 mg m^{-2} s^{-1}). The FG system seemed to have adequate precision for the CO_2 flux measurement at this eutrophic lake. For reference, lake CO_2 emission ranges from −0.051−0.344 mg m^{-2} s^{-1} among the lakes in the world, and roughly 50% of the lakes have mean fluxes that exceed one standard deviation of the zero-gradient test (Table S3, Supporting Information).

The CO_2 flux comparison shows much more scatter than does the latent heat flux comparison, which underscores the difficulty in measuring the CO_2 flux in the lake environment. The R^2 values are 0.00007 ($p > 0.10$) and 0.56 ($p < 0.001$) for the CO_2 and the latent heat flux, respectively. Uncertainty in the density correction is believed to be a major source of the scatter. A random error of 10 W m^{-2} in the sensible heat flux, which is typical of EC measurements, would result in an error of 0.040 mg m^{-2} s^{-1} to the CO_2 WPL density correction term; this error is comparable in magnitude to the mean EC flux (0.020 mg m^{-2} s^{-1}). Additionally, open-path EC is susceptible to the problem of self-heating arising from artificial density fluctuations caused by the heat generated by the EC analyzer.[27] At present, no satisfactory postmeasurement method exists to correct the problem.

The FG system used a closed-path analyzer that does not need correction for the density effect arising from sensible heat flux and from different inlet temperature because the temperature fluctuation within the sampling cell is small, and the air samples from the two inlets were brought to a common temperature.[47] The density effect due to water vapor was dealt with numerically by an empirical function imbedded in the analyzer's data processing firmware. This correction procedure has been thoroughly tested by the manufacturer up to a water vapor concentration of 1 %v. The water vapor mixing ratio was often higher than 1 %v during this experiment. Rella et al.[40] made parallel measurements of CO_2 with the online numerical correction and with cryogenic removal of water vapor using two analyzers of the same type as in this study. Their results can be used to obtain some sense of how the FG flux may have been affected by the residual density effect outside the 1 %v humidity threshold. Over the humidity range of 0.8−1.8 %v, their observed difference shows a slight humidity dependence, at a rate of 0.062 ppm of CO_2 per $\%H_2O$. At a typical water vapor mixing ratio difference of 0.1 %v (Figure 3), the residual density correction error is on the order of 0.006 ppm for the CO_2 difference, which is an order of magnitude lower than the standard deviation of the zero-gradient test (Table 1) and corresponds to a negligibly small CO_2 flux error of 0.0012 mg m^{-2} s^{-1}. The negligible density effects on the FG flux are a major advantage of the closed-path FG method over the open-path EC method. Readers are reminded that the comparison could be different if a closed-path EC instrument was employed instead.

3.4. CH_4 Flux. The FG measurement indicates that the lake was a CH_4 source, while the negative fluxes were associated with experimental uncertainties (Figure 6c). About 80% of the data were positive, and 71% of the positive data were higher in magnitude than one standard deviation of the zero-gradient test (0.029 μg m^{-2} s^{-1}). Although negative fluxes have been reported for other lake systems,[55−57] in the present study, these fluxes were more likely caused by random measurement errors than indicative of CH_4 consumption. These negative fluxes usually occurred in transitional periods when wind direction changed rapidly from bad fetch to good fetch, which resulted in significant time trend of CH_4 concentration within the half-hourly observations. Because of the sequential sampling scheme used, some of the time trend would cause large biases to the gradient measurement.

The study of Rella et al.[40] suggests that the analyzer's in situ water vapor density correction is adequate for the FG application. They show that after the correction, the residual error of the corrected CH_4 mixing ratio has a very weak dependence on the ambient humidity (0.47 ppb per $\%$ H_2O). At the typical H_2O mixing ratio difference of 0.2 %v (Figure 3), the residual water vapor density effect (0.094 ppb) is an order of magnitude smaller than the measurement precision of the FG method (Table 1).

The lake−air CH_4 flux is dependent largely on the C availability of the lake substrate and on the mixing status of the lake water.[16] The CH_4 flux ranges from 0.002−0.017 μg CH_4 m^{-2} s^{-1} in the mesohumic Lake Pääjärvi.[58] Having large amounts of submerged biomass, a boreal beaver pond[30] is a CH_4 source with a seasonal mean flux of 1.3 μg m^{-2} s^{-1}. Hydropower reservoirs can have much higher fluxes than natural lakes due to more submerged dead biomass and particle organic matter input to the sediment. A Swiss hydropower reservoir[21] releases CH_4 at flux intensities of 5.0−10.0 μg CH_4 m^{-2} s^{-1}. Big CH_4 flux (up to 15 μg m^{-2} s^{-1}) events have been observed in Lake Rotsee during lake turnover.[8] The FG system

described here has adequate precision to measure the flux in most of these situations.

In highly eutrophic lakes, organic carbon can come from river runoff and in situ primary production associated with phytoplankton growth. It is reasonable to hypothesize that these two large sources may support strong CH_4 emission to the atmosphere; however, the results of this study do not support such a viewpoint, as shown in Figure 7 where the data

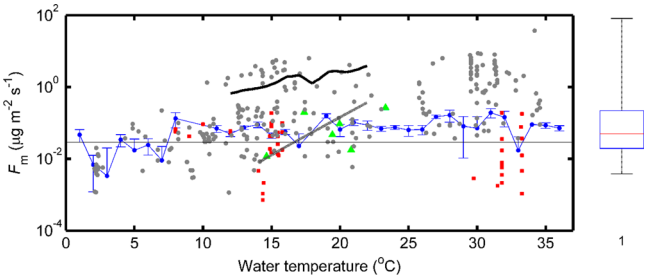

Figure 7. Relationship between F_m and water temperature (T_w). Gray dots, eutrophic water bodies; red squares, oligotrophic water bodies; green triangles, mesotrophic water bodies; solid line, a hydropower reservoir;[21] dashed line, a eutrophic lake;[61] blue dots, this study, with one standard error indicated; thin solid line, the detection limit of the FG system (0.029 μg m^{-2} s^{-1}); box plot, the minimum, 25th percentile, median, 75th percentile, and maximum value of the lake data found in the literature. Sources of the literature data are given in the Supporting Information.

of this study are compared with those found in the literature. In this study, the mean flux is 0.056 μg CH_4 m^{-2} s^{-1} (1.8 g CH_4 m^{-2} year^{-1}) and is very close to the median value (1.6 g CH_4 m^{-2} year^{-1}) of the 86 lake studies reviewed by Bastviken et al.[5] and Ortiz-Llorente.[59]

In the temperature range >15 °C, the present study indicates lower emission flux than those found for other eutrophic lakes. For clarity, our data are bin-averaged according to water temperature. Some of this difference may be caused by different methodologies used. Of the eight eutrophic lake studies included in this comparison, six used the floating chamber method for flux determination. For example, using the floating chamber method, Wang et al.[60] reported a much larger annual mean flux of 74.7 g CH_4 m^{-2} yr^{-1} for the same measurement location in Lake Taihu.

■ ASSOCIATED CONTENT

Supporting Information

Instrument calibration information, a comparison of the water vapor mixing ratio difference between the two air intakes, a comparison of CO_2 flux and CH_4 flux, data used for the relationship between F_m and water temperature, annual methane emissions from lakes worldwide, and lake CO_2 data. This material is available free of charge via the Internet at http://pubs.acs.org.

■ AUTHOR INFORMATION

Corresponding Author

*Phone: (203)432-6271; fax: (203)432-5023; e-mail: xuhui.lee@yale.edu.

Notes

The authors declare no competing financial interest.

■ ACKNOWLEDGMENTS

This research was supported by the National Natural Science Foundation of China (Grants No. 41475141, 41275024); the Natural Science Foundation of Jiangsu Province, China (Grant No. BK2011830); the Ministry of Education of China (Grant No. PCSIRT); and the Priority Academic Program Development of Jiangsu Higher Education Institutions (Grant No. PAPD).

■ REFERENCES

(1) St Louis, V. L.; Kelly, C. A.; Duchemin, É.; Rudd, J. W. M.; Rosenberg, D. M. Reservoir surfaces as sources of greenhouse gases to the atmosphere: A global estimate. *BioScience* **2000**, *50* (9), 766−775.

(2) Cole, J. J.; Prairie, Y. T.; Caraco, N. F.; McDowell, W. H.; Tranvik, L. J.; Striegl, R. G.; Duarte, C. M.; Kortelainen, P.; Downing, J. A.; Middelburg, J. J.; Melack, J. Plumbing the global carbon cycle: Integrating inland waters into the terrestrial carbon budget. *Ecosystems* **2007**, *10*, 171−184.

(3) Battin, T. J.; Luyssaert, S.; Kaplan, L. A.; Aufdenkampe, A. K.; Richter, A.; Tranvik, L. J. The boundless carbon cycle. *Nat. Geosci.* **2009**, *2*, 598−600.

(4) Tranvik, L. J.; Downing, J. A.; Cotner, J. B.; Loiselle, S. A.; Striegl, R. G.; Ballatore, T. J.; Dillon, P.; Finlay, K.; Fortino, K.; Knoll, L. B.; Kortelainen, P. L.; Kutser, T.; Larsen, S.; Laurion, I.; Leech, D. M.; McCallister, S. L.; McKnight, D. M.; Melack, J. M.; Overholt, E.; Porter, J. A.; Prairie, Y.; Renwick, W. H.; Roland, F.; Sherman, B. S.; Schindler, D. W.; Sobek, S.; Tremblay, A.; Vanni, M. J.; Verschoor, A. M.; von Wachenfeldt, E.; Weyhenmeyer, G. A. Lakes and reservoirs as regulators of carbon cycling and climate. *Limnol. Oceanogr.* **2009**, *54* (6 part 2), 2298−2314.

(5) Bastviken, D.; Tranvik, L. J.; Downing, J. A.; Crill, P. M.; Enrich-Prast, A. Freshwater methane emissions offset the continental carbon sink. *Science* **2011**, *331*, 50.

(6) Broecker, W. S.; Peng, T. H. Gas Exchange Measurements in Natural Systems. In *Gas Transfer at Water Surfaces*; Brutsaert, W., Jirka, G. H., Eds.; D. Reidel Publishing Co.: Dordrecht, The Netherlands, 1984; pp 479−495.

(7) Eugster, W.; Kling, G.; Jonas, T.; McFadden, J. P.; Wüest, A.; MacIntyre, S.; Chapin, F. S., III CO_2 exchange between air and water in an Arctic Alaskan and midlatitude Swiss lake: Importance of convective mixing. *J. Geophys. Res.* **2003**, *108* (D12), 4362.

(8) Schubert, C. J.; Diem, T.; Eugster, W. Methane emissions from a small wind shielded lake determined by eddy covariance, flux chambers, anchored funnels, and boundary model calculations: A comparison. *Environ. Sci. Technol.* **2012**, *46*, 4515−4522.

(9) Cole, J. J.; Bade, D. L.; Bastviken, D.; Pace, M. L.; van de Bogert, M. Multiple approaches to estimating air−water gas exchange in small lakes. *Limnol. Oceanogr.: Methods* **2010**, *8*, 285−293.

(10) Gålfalk, M.; Bastviken, D.; Fredriksson, S.; Arneborg, L. Determination of the piston velocity for water−air interfaces using flux chambers, acoustic Doppler velocimetry, and IR imaging of the water surface. *J. Geophys. Res.* **2013**, *118*, 770−782.

(11) Schilder, J.; Bastvinken, D.; van Hardenbroek, M.; Kankaala, P.; Rinta, P.; Stötter, T.; Heiri, O. Spatial heterogeneity and lake morphology affect diffusive greenhouse gas emission estimates of lakes. *Geophys. Res. Lett.* **2013**, *40*, 5752−5756.

(12) Liss, P.; Merlivat, L. Air−Sea Gas Exchange Rates: Introduction and Synthesis. In *The Role of Air−Sea Exchange in Geochemical Cycling*; Baut-Ménard, P., Ed.; D. Reidel Publishing Company: Dordrecht, The Netherlands, 1986; pp 113−127.

(13) Liss, P. S.; Slater, P. G. Fluxes of gases across the air−sea interface. *Nature* **1974**, *247*, 181−184.

(14) Cole, J. J.; Caraco, N. F. Atmospheric exchange of carbon dioxide in a low-wind oligotrophic lake measured by the addition of SF_6. *Limnol. Oceanogr.* **1998**, *43* (4), 647−656.

(15) Upstill-Goddard, R. C.; Watson, A. J.; Liss, P. S.; Liddicoat, M. I. Gas transfer velocities in lakes measured with SF_6. *Tellus* **1990**, *42B*, 364−377.

(16) Bastviken, D.; Cole, J.; Pace, M.; Tranvik, L. Methane emissions from lakes: Dependence of lake characteristics, two regional assessments, and a global estimate. *Global Biogeochem. Cycles* **2004**, *18*, GB4009.
(17) Anderson, D. E.; Striegl, R. G.; Stannard, D. I.; Michmerhuizen, C. M.; McConnaughey, T. A.; LaBaugh, J. W. Estimating lake−atmosphere CO_2 exchange. *Limnol. Oceanogr.* **1999**, *44* (4), 988−1001.
(18) Vesala, T.; Huotari, J.; Rannik, Ü.; Suni, T.; Smolander, S.; Sogachev, A.; Launiainen, S.; Ojala, A. Eddy covariance measurements of carbon exchange and latent and sensible heat fluxes over a boreal lake for a full open-water period. *J. Geophys. Res.* **2006**, *111*, D11101.
(19) Polsenaere, P.; Deborde, J.; Detandt, G.; Vidal, L. O.; Pérez, M. A. P.; Marieu, V.; Abril, G. Thermal enhancement of gas transfer velocity of CO_2 in an Amazon floodplain lake revealed by eddy covariance measurements. *Geophys. Res. Lett.* **2013**, *40*, 1734−1740.
(20) Edwards, G. C.; Neumann, H. H.; den Hartog, G.; Thurtell, G. W.; Kidd, G. E. Eddy correlation measurements of methane fluxes using a tunable diode laser at the Kinosheo Lake tower site during the Northern Wetlands Study (NOWES). *J. Geophys. Res.* **1994**, *99*, 1511−1517.
(21) Eugster, W.; DelSontro, T.; Sobek, S. Eddy covariance flux measurements confirm extreme CH_4 emission from a Swiss hydropower reservoir and resolve their short-term variability. *Biogeosciences* **2011**, *8*, 2815−2831.
(22) Miller, S. D.; Marandino, C.; Saltzman, E. S. Ship-based measurement of air−sea CO_2 exchange by eddy covariance. *J. Geophys. Res.* **2010**, *115*, D02304.
(23) Lee, X.; Massman, W. J. A perspective on thirty years of the Webb, Pearman, and Leuning density correction. *Boundary-Layer Meteorol.* **2011**, *139*, 37−59.
(24) Edson, J. B.; Hinton, A. A.; Prada, K. E.; Hare, J. E.; Fairall, C. W. Direct covariance flux estimates from mobile platforms at sea. *J. Atmos. Oceanic Technol.* **1998**, *15*, 547−562.
(25) Blomquist, B. W.; Huebert, B. J.; Fairall, C. W.; Faloona, I. C. Determining the sea−air flux of dimethylsulfide by eddy correlation using mass spectrometry. *Atmos. Meas. Technol.* **2010**, *3*, 1−20.
(26) Norman, M.; Rutgersson, A.; Sørensen, L. L.; Sahlée, E. Methods for estimating air−sea fluxes of CO_2 using high-frequency measurements. *Boundary-Layer Meteorol.* **2012**, *144*, 379−400.
(27) Burba, G. G.; McDermitt, D. K.; Grelle, A.; Anderson, D. J.; Xu, L. Addressing the influence of instrument surface heat exchange on the measurements of CO_2 flux from open-path gas analyzers. *Global Change Biol.* **2008**, *14*, 1854−1876.
(28) Baldocchi, D. D.; Hicks, B. B.; Meyers, T. P. Measuring biosphere−atmosphere exchanges of biologically related gases with micrometeorological methods. *Ecology* **1988**, *69* (5), 1331−1340.
(29) Meyers, T. P.; Hall, M. E.; Lindberg, S. E.; Kim, K. Use of the modified Bowen-ratio technique to measure fluxes of trace gases. *Atmos. Environ.* **1996**, *30* (19), 3321−3329.
(30) Roulet, N. T.; Crill, P. M.; Comer, N. T.; Dove, A.; Boubonniere, R. A. CO_2 and CH_4 flux between a boreal beaver pond and the atmosphere. *J. Geophys. Res.* **1997**, *102* (D24), 29313−29319.
(31) Zappa, C. J.; Raymond, P. A.; Terray, E. A.; McGillis, W. R. Variation in surface turbulence and the gas transfer velocity over a tidal cycle in a macro-tidal estuary. *Estuaries* **2003**, *26* (6), 1401−1415.
(32) Dyer, A. J.; Hicks, B. B. Flux-gradient relationships in the constant flux layer. *Quart. J. R. Met. Soc.* **1970**, *96*, 715−721.
(33) Simpson, I. J.; Thurtell, G. W.; Kidd, G. E.; Lin, M.; Demetriades-Shah, T. H.; Flitcroft, I. D.; Kanemasu, E. T.; Nie, D.; Bronson, K. F.; Neue, H. U. Tunable diode laser measurements of methane fluxes from an irrigated rice paddy field in the Philippines. *J. Geophys. Res.* **1995**, *100* (D4), 7283−7290.
(34) Dyer, A. J. A review of flux−profile relationships. *Boundary-Layer Meteor.* **1974**, *7*, 363−372.
(35) Crosson, E. R. A cavity ring-down analyzer for measuring atmospheric levels of methane, carbon dioxide, and water vapor. *Appl. Phys.* **2008**, *B 92*, 403−408.
(36) Chen, H.; Winderlich, J.; Gerbig, C.; Hoefer, A.; Rella, C. W.; Crosson, E. R.; Van Pelt, A. D.; Steinbach, J.; Kolle, O.; Beck, V.; Daube, B. C.; Gottlieb, E. W.; Chow, V. Y.; Santoni, G. W.; Wofsy, S. C. High-accuracy continuous airborne measurements of greenhouse gases (CO_2 and CH_4) using the cavity ring-down spectroscopy (CRDS) technique. *Atmos. Meas. Technol.* **2010**, *3*, 375−386.
(37) Karion, A.; Sweeney, C.; Wolter, S.; Newberger, T.; Chen, H.; Andrews, A.; Kofler, J.; Neff, D.; Tans, P. Long-term greenhouse gas measurements from aircraft. *Atmos. Meas. Technol.* **2013**, *6*, 511−526.
(38) Welp, L. R.; Keeling, R. F.; Weiss, R. F.; Paplawsky, W.; Heckman, S. Design and performance of a Nafion dryer for continuous operation at CO_2 and CH_4 air monitoring sites. *Atmos. Meas. Technol.* **2013**, *6*, 1217−1226.
(39) Wastine, B.; Kaiser, C.; Vuillemin, C.; Lavrič, J. V.; Schmidt, M.; Ramonet, M. Evaluation of the Picarro EnviroSense 3000i analyzer (now called G1301) for continuous CO_2/CH_4 measurements. In *Geophysical Research Abstracts of European Geosciences Union General Assembly*; EGU General Assembly: Vienna, Austria, April 19 − 24, 2009; p 2562.
(40) Rella, C. W.; Chen, H.; Andrews, A. E.; Filges, A.; Gerbig, C.; Hatakka, J.; Karion, A.; Miles, N. L.; Richardson, S. J.; Steinbacher, M.; Sweeney, C.; Wastine, B.; Zellweger, C. High accuracy measurements of dry mole fractions of carbon dioxide and methane in humid air. *Atmos. Meas. Technol.* **2013**, *6*, 837−860.
(41) Griffith, D. W. T.; Leuning, R.; Denmead, O. T.; Jamie, I. M. Air−land exchanges of CO_2, CH_4, and N_2O measured by FTIR spectrometry and micrometeorological techniques. *Atmos. Environ.* **2002**, *36*, 1833−1842.
(42) Lee, X.; Liu, S.; Xiao, W.; Wang, W.; Gao, Z.; Cao, C.; Hu, C.; Hu, Z.; Shen, S.; Wang, Y.; Wen, X.; Xiao, Q.; Xu, J.; Yang, J.; Zhang, M. The Taihu eddy flux network: An observational program on energy, water, and greenhouse gas fluxes of a large freshwater lake. *Bull. Am. Meteor. Soc.* **2014**, in press (http://dx.doi.org/10.1175/BAMS-D-13-00136.1).
(43) Hu, W. P.; Jørgensen, S. E.; Zhang, F. B.; Chen, Y. G.; Hu, Z. X.; Yang, L. Y. A model on the carbon cycling in Lake Taihu, China. *Ecol. Modell.* **2011**, *222*, 2973−2991.
(44) Hsieh, C.; Katul, G.; Chi, T. An approximate analytical model for footprint estimation of scalar fluxes in thermally stratified atmospheric flows. *Adv. Water Resour.* **2000**, *23*, 765−772.
(45) Xiao, W.; Liu, S.; Wang, W.; Yang, D.; Xu, J.; Cao, C.; Li, H.; Lee, X. Transfer coefficients of momentum, heat, and water vapor in the atmospheric surface layer of a large freshwater lake. *Boundary-Layer Meteorol.* **2013**, *148*, 479−494.
(46) Lee, X.; Finnigan, J.; Paw, U. K. T. Coordinate Systems and Flux Bias Error. In *Handbook of Micrometeorology: A Guide for Surface Flux Measurement and Analysis*; Lee, X., Massman, W., Law, B., Eds.; Kluwer Academic Publishers: New York, 2004; pp 33−66.
(47) Webb, E. K.; Pearman, G. I.; Leuning, R. Correction of flux measurements for density effects due to heat and water vapor transfer. *Quart. J. R. Met. Soc.* **1980**, *106*, 85−100.
(48) Serrano-Ortiz, P.; Kowalski, A. S.; Domingo, F.; Ruiz, B.; Alados-Arboledas, L. Consequences of uncertainties in CO_2 density for estimating net ecosystem CO_2 exchange by open-path eddy covariance. *Boundary-Layer Meteorol.* **2008**, *126*, 209−218.
(49) Xiao, W.; Lee, X.; Liu, S.; Hu, X.; Wang, W.; Lee, H.; Xiao, Q. The CH_4, CO_2, and H_2O flux at the lake−air interface based on the gradient diffusion method. 2012 AGU Fall Meeting, San Francisco, CA, Dec 3−7, 2012.
(50) Chan, A. S. K.; Prueger, J. H.; Parkin, T. B. Comparison of closed-chamber and Bowen-ratio methods for determining methane flux from peatland surfaces. *J. Environ. Qual.* **1998**, *27*, 232−239.
(51) Kroon, P. S.; Hensen, A.; Jonker, H. J. J.; Ouwersloot, H. G.; Vermeulen, A. T.; Bosveld, F. C. Uncertainties in eddy covariance flux measurements assessed from CH_4 and N_2O observations. *Agric. Forest Meteorol.* **2010**, *150*, 806−816.
(52) Duc, N. T.; Silverstein, S.; Lundmark, L.; Reyier, H.; Crill, P.; Bastviken, D. Automated flux chamber for investigating gas flux at water−air interfaces. *Environ. Sci. Technol.* **2012**, *47*, 968−975.

(53) Kaimal, J. C.; Finnigan, J. J. *Atmospheric Boundary Layer Flows: Their Structure and Measurement*; Oxford University Press: Oxford, U.K., 1994.
(54) Willmot, C. J. On the Evaluation of Model Performance in Physical Geography. In *Spatial Statistics and Models*; Gaile, G. L., Willmot, C. J., Eds.; D. Reidel Publishing Company: Dordrecht, The Netherlands, 1984; pp 443−460.
(55) Chen, H.; Wu, N.; Yao, S.; Gao, Y.; Zhu, D.; Wang, Y.; Xiong, W.; Yuan, X. High methane emissions from a littoral zone on the Qinghai−Tibetan Plateau. *Atmos. Environ.* **2009**, *43*, 4995−5000.
(56) Juutinen, S.; Alm, J.; Martikainen, P.; Silvola, J. Effects of spring flood and water level draw-down on methane dynamics in the littoral zone of boreal lakes. *Freshwater Biol.* **2011**, *46*, 855−869.
(57) Zhu, R.; Liu, Y.; Xu, H.; Huang, T.; Sun, J.; Ma, E.; Sun, L. Carbon dioxide and methane fluxes in the littoral zones of two lakes, East Antarctica. *Atmos. Environ.* **2010**, *44*, 304−311.
(58) Bellido, J. L.; Tulonen, T.; Kankaala, P.; Ojala, A. CO_2 and CH_4 fluxes during spring and autumn mixing period in a boreal lake (Pääjärvi, southern Finland). *J. Geophys. Res.* **2009**, *114*, G04007.
(59) Ortiz-Llorente, M. J.; Alvarez-Cobelas, M. Comparison of biogenic methane emissions from unmanaged estuaries, lakes, oceans, rivers, and wetlands. *Atmos. Environ.* **2012**, *59*, 328−337.
(60) Wang, H.; Lu, J.; Wang, W.; Yang, L.; Yin, C. Methane fluxes from the littoral zone of hypereutrophic Taihu Lake, China. *J. Geophys. Res.* **2006**, *111*, D17109.
(61) Takita, M.; Sakamoto, M. Methane flux in a shallow eutrophic lake. *Proc. Int. Assoc. Theor.* **1993**, *25*, 822−826.